Low thermal sensitivity grating devices based on ex-45° tilting structure capable of forward propagating cladding modes coupling

Kaiming Zhou, Lin Zhang, Xianfeng Chen, Ian Bennion

Photonic Research Group, Aston University, Birmingham, B4 7ET, United Kingdom
Phone +44(0)1212043504, k.zhou@aston.ac.uk

Abstract: We describe a detailed investigation on tilted fiber Bragg grating (TFBG) structures with tilted angles exceeding 45°. In contrast to the backward mode coupling mechanism of Bragg gratings with normal and small-tilting structures, the ex-45° TFBGs facilitate the light coupling to the forward propagating cladding modes. We have theoretically and experimentally examined the mode coupling transition of TFBGs with small, medium and large tilt angles. In particular, we have conducted experiments to investigate the spectra and far field distribution, and temperature, strain and refractive index sensitivities of ex-45° devices. It has been revealed that these ex-45° gratings exhibit ultra-low thermal sensitivity. As in-fiber devices, they may be superior to conventional Bragg and long period gratings when the low thermal cross sensitivity is required.

Key words: Optical gratings Fiber Bragg gratings Optical fiber radiation effects Coupled mode analysis optical biosensors

1. Introduction

Mode couplings assisted by fiber Bragg grating (FBG) and long-period grating (LPG) structures have been extensively studied over the last decade [1,2]. The reflection type of devices based on FBG configuration utilizes the light coupling between the forward- and backward-propagating core modes in the fiber, whereas the loss type of filters based on LPG structure is realized by coupling the light between the forward-propagating core and cladding modes. A range of applications and devices utilizing FBGs and LPGs have been extensively investigated and developed. However, another type of fiber gratings with tilted index fringes capable of light coupling from core to cladding and radiation modes is much less exploited. Erdogan and Sipe were the first to give a detailed treatment to tilted fiber Bragg grating (TFBG) structures in 1996 [3]. Since then, a handful of application devices utilizing TFBGs were reported, including in-fiber spectrometer [4-6], WDM channel monitoring [7], gain flattening of EDFAs [8] and optical sensor interrogation [9-11]. Due to their exceptional polarization sensitivity, TFBGs have also

been implemented as in-line polarimeter [12,13], polarization dependent loss equalizer [14,15] and, recently, high-extinction-ratio polarizers [16]. However, in all these literatures, tilting angles of all the gratings are at most 45° and, therefore, the light is only coupled from the forward-propagating core mode to backward-propagating cladding modes or radiation modes. To our knowledge, few theoretical and no experimental studies have been conducted to examine the TFBGs with tilted structures larger than 45°. With such structures, the light coupling may occur between forward-propagating core and cladding modes. Conventionally, forward cladding mode coupling only works with LPGs, which are more sensitive to environmental parameters than FBGs. In comparison with FBGs, LPGs have relative long device size and broad spectral width, which instigate low stability and poor spectral resolution. Thereby, if forward cladding modes coupling could be realized by TFBGs, then these devices may offer advantageous spectral-characteristics and device functions over both conventional FBGs and LPGs.

In this paper we report a detailed experimental investigation on TFBGs of ex-45° structures, revealing their forward-propagating cladding mode coupling function and temperature, strain and refractive index sensitivity characteristics. In addition, the mode coupling regimes and associated phase match conditions for TFBGs of small, medium and large tilt angles, and the exact range of radiation mode coupling will be discussed

This paper is constructed as follows. In section II, we present a general vectorial phase match condition analysis for TFBGs with tilted structures <, = and > 45°, corresponding to the backward-, out- and forward-coupling regimes. We then analyze the critical conditions and the radiation mode out-coupling ranges for TFBGs surrounded by air and water solution. Section III describes the fabrication and characterization of ex-45° TFBGs and shows distinct transmission spectra of three TFBGs with tilted structures at 65°, 69° and 81°. In section IV, we report on the temperature, strain and refractive index sensitivity characteristics of ex-45° TFBGs, revealing their low thermal and high refractive index sensitivities. Finally, we draw conclusions in Section V.

2. Phase match condition and mode coupling range of TFBG

When light propagating in the core mode meets a section of TFBG, it is firstly radiated out of the fiber core by the grating and then travels in the cladding until it strikes on the boundary of the cladding. The first process has been theoretically analyzed in detail in several papers utilizing Green Function method (also called Volume Current method) by adopting a cladding with infinite thickness [17,18]. Although using this method, various aspects of the radiation can be calculated, such as the spread of beam, spectrum and the strength, it is much more straightforward to examine the coupled mode propagation employing its derivation – the phase match condition[19]. We will herein use the vectorial model of the phase match condition to identify the mode coupling regimes of TFBGs with tilt angles <45°, = 45° and >45°, respectively, and calculate the coupling ranges for cladding and radiation modes by taking the total internal reflection (TIR) into consideration.

A. Phase match conditions for TFBGs of tilt angles less and larger than 45°

When a beam of a certain bandwidth encounters a TFBG in the fiber, its components are radiated out of the fiber core in different directions with different strengths. The strongest light coupling takes place at the phase match condition

$$\mathbf{K_R} = \mathbf{K_{core}} + \mathbf{K_G}, \tag{1}$$

where $\mathbf{K_R}$, $\mathbf{K_{core}}$ and $\mathbf{K_G}$ are wave vectors of the radiated light, core mode and grating itself, respectively. In a general case, we may neglect the amplitude difference between $\mathbf{K_R}$ and $\mathbf{K_{core}}$, since the refractive indices of the core and the cladding are very close. Fig. 1a, b and c illustrate graphically the phase match conditions for TFBGs with tilt angles < 45°, = 45° and > 45°, respectively. From the figures we can see that under the phase match condition, the amplitudes of $\mathbf{K_R}$ and $\mathbf{K_{core}}$ are related as

$$K_R = \frac{K_G}{2\cos(\delta)} \quad (\theta = \pi - 2\delta), \tag{2}$$

where θ and δ are the radiation and tilted angle of the TFBG, respectively. For a given grating with specified δ and K_G, we can identify the direction (θ) and wavelength ($2\pi/K_R$) of the main beam $\mathbf{K_R}$ from Eq.2. On the other hand, we can also use Eq.2 to design a grating with particular tilt structure for light at certain wavelength to be radiated in a desired direction.

From the wave vectors drawn in Fig. 1a, we see that the main beam, $\mathbf{K_R}$, satisfies the phase match condition, thus it will be strongly coupled at θ direction, whereas the non-phase matched light, $\mathbf{K'_R}$, will be weakly coupled at θ′ (the angle between $\mathbf{K'_R}$ and x-axis) direction, at which the mismatch among $\mathbf{K'_R}$, $\mathbf{K_{core}}$ and $\mathbf{K_G}$ is minimal. From Fig.1a, we can derive the relationship between θ′ and grating parameters δ and K_G as

$$\mathrm{ctan}\left(\theta'\right)=\frac{K'_R}{K_G}\frac{1}{\sin(\delta)}-\mathrm{ctan}\left(\delta\right) \tag{3}$$

If $\delta < 45°$, the x-components of the radiated beams of $\mathbf{K_R}$ and $\mathbf{K'_R}$ are all in opposite direction to x, indicating that those radiated lights will be coupled from forward-propagating core mode into the backward-propagating modes. From Eq. 2 we note if $\delta = 45°$ θ will be 90°, thus all the phase matched light will be completely radiated out of the fiber, as shown in Fig. 1b. In the third case, as shown in Fig. 1c where $\delta > 45°$, we clearly see that the x-components of $\mathbf{K_R}$ and $\mathbf{K'_R}$ are in positive x-direction, indicating that the light will be coupled into the forward-propagating cladding modes.

B. Critical condition and mode coupling range

One of the unique functions of TFBGs is to couple the light out from the fiber. This functionality has been utilized for several types of device. The most attractive TFBG device is the in-fiber WDM spectrum analyzer [4-6], which is a low-cost alternative to lab-based bulky and expensive optical spectrum analyzers and can be potentially incorporated into real application systems. However, due to the TIR effect of the cladding boundary, especially with the air, the light is mostly confined in the cladding modes for TFBGs with relative small (or large) tilted angles. To tap out the light from fiber, the TFBG has to be immersed in the index matching gel or housed with an adaptive optics of similar index to the fiber cladding, effectively increasing the thickness of the cladding to facilitate the radiation mode coupling. This obviously imposes difficulty and restriction on device packaging and applications. However, when $\delta < 45°$ and $\delta > 45°$, the light may not be entirely coupled into the cladding modes, and there is a range where the light can be radiated out from the fiber. The range for radiation mode coupling depends on the critical angle of the fiber, which is defined as $\alpha_c = \arcsin(n_1/n_2)$, where n_1 and n_2 are refractive indices of the surrounding medium and cladding, respectively.

If we designate the incident angle as ϕ, as shown in Fig. 1a, for the phase matched beam, $\mathbf{K_R}$, ϕ is related to the tilt angle δ by $\underline{\phi = \pi/2 - 2\cdot\delta}$. If $|\phi| < \alpha_c$ we have a radiation mode coupling range given by $\delta_{1c} < \delta < \delta_{2c}$, where δ_{1c} and δ_{2c} can be calculated as

$$\delta_{1c} = \tfrac{1}{2}\left(\tfrac{\pi}{2} - \alpha_c\right), \ \delta_{2c} = \tfrac{1}{2}\left(\tfrac{\pi}{2} + \alpha_c\right). \tag{4}$$

Considering a case where the fiber is surrounded by vacuum (air), we calculate the critical angle $\alpha_c = 43.8°$. Thus, to realize radiation mode coupling, the grating tilt angle δ should be designed in the range from 23.1° to 66.9°. If we change the surrounding to the water based solution (n ~ 1.33), the radiation mode coupling range is enlarged and becomes 11.5° to 78.5°.

Fig. 2a, b and c clearly illustrate the ranges for three mode coupling regimes. When $\delta < \delta_{1c}$, the light bounces back from the boundary and is coupled into the cladding modes propagating in the backward-direction. In this case, a series of relatively dense resonances can be observed from the transmission spectrum, as shown in Fig. 2d. If the tilted structure satisfies $\delta_{1c} < \delta < \delta_{2c}$ the light will be tapped out from the side of the fiber. In this regime, the transmission spectrum of the TFBG should be a smooth loss profile of radiation mode (leaky mode) coupling. Our previous theoretical and experimental study shows that the radiation profile is strongly polarization dependent [16]. For a unique case where $\delta = 45°$, the s-polarized light will strongly be coupled out from the fiber whereas the p-polarized light propagates in the fiber. Fig. 2e shows the loss profile of s-polarized light for a 45°-tilted structure. If the tilt angle is increased further to $\delta > \delta_{2c}$ light will be trapped again in the fiber cladding modes, but propagating in the forward-direction. In this case, we also see a series of comb-like resonances, but with slightly larger mode spacings, as shown in Fig. 2f. Note, the relatively dense and sparse spectra for $\delta < \delta_{1c}$ and $> \delta_{2c}$ shown in Fig. 2d and 2f are the direct result of relative small and large periods required to satisfy the phase match conditions for the two cases.

To date, there is almost no report on experiment work of TFBGs operating in forward cladding mode regime. We have fabricated ex-45° TFBGs and investigated their spectral, far-field and sensitivity characteristics, and the detailed results will be discussed in the sections below.

3. Fabrication and characterization of ex-45° TFBGs

The ex-45° TFBGs were UV-inscribed in hydrogenated B/Ge co-doped and standard telecom fibers employing the scanning phase mask technique using a frequency doubled cw Ar$^+$ laser. The tilted structure was realized by rotating the phase mask in the fabrication system. Two custom-designed masks of periods 1.8μm from QPS and 6.6μm from Edmund Optics Ltd were used for ex-45° TFBG fabrication. Two TFBGs of 3.5mm long with internal tilt fringes at 65° and 69° and one TFBG of 15mm long with internal tilt angle at 81° were UV-inscribed using 1.8μm and 6.6μm masks, respectively. The first two gratings were designed to investigate the forward cladding mode coupling around 650-800 in air, and the third grating was specially for 1550nm in solutions of refractive indices >1.33. In the UV-inscription system, a 10mm cylindrical lens was used to focus the 100mw laser beam onto the fiber core. The focused beam was scanned along the fiber at 0.07mm/sec by a linearly-motorized translation stage, and in order to increase the index modulation, multiple scans had been applied.

We first examined the grating structures using a high resolution microscope (Axioskop 2 of Carl Zeiss). Fig. 1d shows the image of the tilted fringes of the 65°-TFBG observed using the microscope. The tilted angle of the fringes is measured at 65.62° (155.62°-90°) which is in good agreement with the design parameter.

According to the phase match condition and mode coupling range discussed in section 2, we calculate that the first structure is $< \delta_{2c}$(66.9°), thus, should tap out the light in 830nm region, while the second and the third gratings are $> \delta_{2c,}$ should generate forward coupled cladding mode resonances ranging around 650nm and 1550nm, respectively. In the experiment, the transmission spectrum of 65°-TFBG was examined for the wavelength range from 790nm to 870nm using an 820nm LED. As clearly shown in Fig. 3a, no cladding resonance but only a smooth loss profile is apparent in this range, indicating the light was tapped out from the fiber (note: the slope on the loss profile is due to non-uniform intensity of the LED). We then measured this grating using a white light source at shorter wavelength side from 600nm to 700nm. As expected, for this non phase matching wavelength range, the light is confined in the forward cladding modes. Thus, we see cladding mode resonances with 5nm spacing, as shown in Fig. 3b.

Fig. 3c depicts the transmission spectrum of 69°-TFBG from 600nm to 650nm. Since its angle 69° $> \delta_{2c,}$ the light is coupled to forward cladding modes, as we see a series of resonances with a spacing of ~6nm in this range. However, a noticeable dual-peak feature is apparent on this

spectrum, and it can be seen later that this feature is much more pronounced for 81°-TFBG. It may be expected that the largely tilted fringes will increases the birefringence of the fiber, thus resulting in the light coupling to two sets of modes of two polarization states. This was experimentally verified on 81°-TFBG as will be described later. We then submerged 69°-TFBG into water and saw all the resonances disappeared. This was expected, as its mode coupling has been shifted to the radiation range (69°<78.5°).

The 81°-tilted TFBG, thus, should enable the light to be coupled to forward cladding modes in the water based solution at 1550nm. We measured the spectral response of this grating in the range from 1200nm to 1700nm. Fig. 4a depicts its transmission spectrum, clearly showing a set of comb-like resonances with much more pronounced dual-peak feature. The relative small spacing and narrow peaks manifest that these resonances are the coupling to the high order cladding modes. In a close examination, we can see that the spacing between adjacent and paired peaks are mode order dependent: they are ~53nm and 7nm for the highest (close to 1700nm) and ~40nm and 5nm for the lowest (near 1200nm) order modes, respectively. As shown in Fig. 4a, the strengths of the dual peaks are around 3dB, indicating equal amount of the light is coupled into each of the paired modes. We then inserted a polarizer and polarization controller in the measurement system to select polarization state of the probe light. One of the paired peaks around 1525nm was measured in a zoomed range. As shown in Fig. 4b, with random polarization, we see two 3-dB peaks, and when the light is switched to either polarization, one of the peaks disappears while the other grows into a strong peak of 14dB attenuation. The polarization effect induced spectral separation between the paired peaks is about 6nm, giving an estimated birefringence of ~10^{-4}.

We further investigated the far-field distribution of 69°-TFBG to verify the coupling to the forward-propagating cladding modes. Light from a He-Ne laser was lunched into the grating fiber and into a bare sample fiber for comparison. The far-field patterns were examined on a screen. At 633nm, this fiber should support multiple modes. In order to eliminate mode mixing, the lengths of the grating and the sample fibers were cut to 30cm. Fig. 5 shows the recorded far-field patterns from the experiment. Fig. 5a is from the grating fiber when its grating was exposed to air. Apparently, the far-field pattern consists of a series of rings, obviously associated with the high order cladding modes. To prove that these modes are propagating in the cladding instead of

the core, we examined the evolution of the far-field pattern when the grating was immersed in index matching gel. As shown in Fig. 5b, the pattern evolves into a small bright spot, since the light in the cladding now is tapped out from the side of the fiber via radiation, leaving only residue light in the core. The far-field pattern from the bare fiber sample showed a bright spot on the screen (Fig. 5c), indicating that the light was propagating mainly in the low order core mode.

4. Temperature, strain and refractive index sensitivity characteristics of ex-45° TFBGs

To evaluate the potential of these gratings for applications in sensing, we have investigated the sensitivity properties of ex-45° TFBGs in respect to temperature, strain and surrounding refractive index (SRI).

A. Thermal property of ex-45° TFBG

The 69°- and 81°-tilted FBGs were investigated for their thermal sensitivities. The 69°-TFBG was heated up from room temperature to 50°C in an elevation step of 5°C, and the temperature-induced spectral evolution was monitored *in-situ*. Fig. 6a shows the thermal responses of eight paired cladding modes of 69°-TFBG; the wavelengths of the resonances are almost unchanged for elevated temperatures, indicating it is thermally insensitive. We then heated up 81°-TFBG from 0°C to 70°C also in 5°C increment and monitored its transmission spectrum. Fig. 6b plots the wavelength shifts against temperature for the two paired resonances of the highest and the lowest order modes. The four measured peaks all exhibit a linear thermal response, showing temperature sensitivities 3.3pm/°C and 3.8pm/°C for the former and 7.5pm/°C and 7.8pm/°C for the latter pair modes, respectively. The former values are only a half of the latter, indicating that the thermal sensitivity deceases with mode order. Noticeably, these thermal sensitivity values are at least a order of magnitude lower than that of conventional LPGs, and even also lower than that (~10pm/°C) of normal FBGs.

The marked difference in thermal properties between conventional LPGs and ex-45° TFBGs may be explained from the amplifying factor of the grating period size. The phase match condition: $\lambda = (n_{core} - n_{clad}) \Lambda$ is the same for both LPG and ex-45° TFBG, as they are the forward coupling devices. When temperature changes, both n_{core} and n_{clad} change due to thermal-optical effect but with similar rates, thus resulting in a small change in $n_{core} - n_{clad}$ .The

difference in n_{clad} for high-order and low-order cladding modes is also too small to consider. From the phase match condition, we then see the period Λ is the dominant factor on thermal-induced wavelength shift. From the mask periods and tilt angles, we can calculate that the grating periods along the fiber axis are 1.8μm for 69°-TFBG and 28μm for 81°-TFBG. Thus, their thermal sensitivities can be expected at least a order of magnitude lower than that of conventional LPGs of typical periods 300 - 500μm. However, the optic-thermal effect on n_{core} and n_{clad} will have a cancellation result in the forward coupling regime ($n_{core} - n_{clad}$) instead of an adding effect in the backward coupling regime ($n_{core} + n_{clad}$). Thus, we see lower temperature sensitivity of the ex-45° TFBGs than that of FBGs with normal and small tilted structures.

B. Strain sensitivity

We also carried out an experiment to examine the strain response of 81°-TFBG. The grating fiber was mounted on two metal block holders with one of which fitted with a micrometer driver. The strain from 0 to 2000με was applied to the grating by stretching the fiber, and the wavelength shifts for all the peaks were recorded. Fig. 7a plots the wavelength shift against strain for one of the dual peaks around 1680nm. The plot exhibits a linear relation, giving a strain coefficient of ~ -1.8pm/με, which is slightly higher in value than that (1pm/με at around 1550nm) of normal FBGs. It should be pointed out that the strain coefficient is negative, i.e. the resonant peak moves to shorter wavelength side with increasing strain. This is contrary to normal FBGs but in agreement with LPGs of relatively small periods [20]. Fig. 7b plots the strain coefficient versus the peak-number for eleven paired peaks of the grating. We see that the strain sensitivity also increases with mode order, and one set of the polarized modes has higher strain coefficients than the other set.

C. SRI sensitivity

Of a particular interest in implementing optical biosensor, we wish to know the refractive index sensitivity of ex-45° TFBGs. 81°-tilted TFBG was measured for SRI induced wavelength changes using a set of index matching gels with refractive index ranging from 1.31 to 1.40. It was noted in the experiment that as soon as the grating was submerged in the index gel, each paired peak evolved into one strong resonance. This may be caused by the reducing phase difference between the *p-* and *s-light* at the cladding boundary. Fig. 8 plots the SRI induced shifts

for the two merged peaks at the shortest and longest wavelength side, showing clearly that when the SRI changes from 1.3 to 1.4, the shift reaches almost 15nm for the peak close to 1200nm and increases to 30nm for the one near 1700nm. We see from the figure that the SRI sensitivity of 81°-TFBG exhibits a nonlinear characteristic, and increases dramatically for the high order mode. The average index sensitivity of the peak near 1700nm is ~340nm/RIU around 1.33, which is 6 times higher than that of the conventional LPGs of 400μm period [21]. With a standard optical interrogation system of resolution 0.1 nm, this TFBG can be used to detect SRI change as small as 3×10^{-4}. Although we did not carry out the measurement beyond n >1.4 region, from the trends we can see that the resolution and sensitivity should be even higher in this region.

5. Conclusions

We have systematically analyzed the mode coupling conditions for forward- and backward-cladding and radiation mode coupling regimes in TFBGs with structures tilted at >, < and = 45°, and identified a range ($\delta_{1c} < \delta < \delta_{2c}$) of radiation mode coupling. The structures with tilt angles inside of this range will be tapped out from the side of the fiber and outside will facilitate light coupling into cladding modes propagating either in backward or forward direction. Experimentally, we have fabricated ex-45° TFBGs and investigated their spectral and far-field distribution, showing clearly the light coupling to the forward cladding modes of high orders. The thermal property evaluation indicates that the ex-45° TFBGs have significantly low thermal cross-sensitivity compared to conventional LPGs and FBGs of normal and small tilted structures. The SRI sensitivity investigation shows that the coupled forward cladding modes in 81°-TFBG possess marked high SRI sensitivity, especially in the refractive index range close to 1.33. Together with their feature of narrow spectral resonances, ex-45° TFBGs could be desirable in-fiber devices offering unique functionalities for applications in optical signal processing and sensing.

Reference:

1. T.Erdogan, "Fiber Grating Spectra," *J.Lightw. Technol.*, vol 15, no.8, pp.1277-1294, Aug.1997
2. R. Kashyap, "Fiber Bragg Grating", Academic Press, 1999
3. T.Erdogan, J.E.Sipe, "Tilted fiber phase gratings", *J. Opt. Soc. Am. A*, vol. 13, pp. 296-313, Feb.1996.
4. G.Meltz, W.W.Morey, and W.H.Glenn, "In-fiber Bragg grating tap", in *Optical Fiber Communication Conference*, Vol. 1 of 1990 OSA Technical Digest Series (Optical Society of America, Washington, D.C., 1990), pp. 30
5. J.L.Wagener, T.A.Strasser, J.R.Pedrazzani, J.Demarco and D.J.Digivanni, "Fiber Grating Optical Spectrum Analyzer Tap", in *ECOC'97,* pp 65-68,1997
6. K.S.Feder, P.S.Westbrook, J.Ging, P.I.Reyes, and G.E.Carver, "In-Fiber Spectrometer Using Tilted Fiber Gratings", *IEEE Photon. Technol. Lett.*, vol.15, no.7, pp.933-935, 2003
7. R.S.Westbrook, K.S.Feder, P.I.Reyes, P.Steinvurzel, B.J.Eggleton, R.G.Ernst, L.A.Reith,and D. M. Gill," Application of fiber Bragg grating filter/tap module to a wavelength-locked low-chirp directly-modulated 10Gb/s Rz transmitter", in *Optical Fiber Communication Conference*, (Anaheim, California, 2002), Paper ThGG49, pp.680-682
8. R.Kashyap, R.Wyatt, and R.J.Campbell, "Wideband gain flattened erbium fibre amplifier using a photosensitive fibre blazed grating", *Electron. Lett.*, vol.29, no.22, pp. 154-156, 1993
9. César Jáuregui, Antonio Quintela, José Miguel López-Higuera, "Interrogation unit for fiber Bragg grating sensors that uses a slanted fiber grating", *Opt. Lett.*, vol.29,no.7, pp.676-678 2004
10. C. Jáuregui, J. Miguel López-Higuera, and A. Quintela, "Interrogation of interferometric sensors with a tilted fiber Bragg grating," *Opt. Express*, vol.12, no.23, pp.5646-5654, 2004
11. Y.Liu, L.Zhang, I.Bennion, "Fabricating fibre edge filters with arbitrary spectral response based on tilted chirped grating structures", *Meas. Sci. Tech.*, vol.10, L1-L3 1999
12. P.S.Westbrook, T.A.Strasser, T.Erdogan, "In-line polarimeter using blazed fiber gratings", *IEEE Photon. Technol. Lett.*, vol.12, no.10, pp.1352 – 1354, 2000
13. J. Peupelmann, E. Krause, A. Bandemer and C. Schäffer, "Fibre-polarimeter based on grating taps", *Electron. Lett.*, vol.38, no.21, pp.1248-1250, 2002
14. S.L.Mihailov, R.B.Walker, T.J.Stocki, D.C.Johnson, "Fabrication of tilted fibre-grating polarisation-dependent loss equaliser", *Electronics Letters*, vol.37 ,pp.284 – 286, 2001
15. P.I.D.C.Reyes, P.S.Westbrook, "Tunable PDL of Twisted-Tilted Fiber Gratings", *IEEE Photon. Technol. Lett.*, vol.15, no.6, pp.828-830 2003
16. K.Zhou, X.Chen, A.G.Simpson, L.Zhang, I.Bennion,"High extinction ratio in-fiber polarizer based on a 45°-tilted fiber Bragg grating"*, in *Optical Fiber Communication Conference*, (Anaheim, California, 2005), paper OME22
17. Y Li, M Froggatt, T Erdogan, "Volume current method for analysis of tilted fiber gratings," *J. Lightw. Technol.* vol. 19, no 10, pp. 1580-1591, 2001
18. M.J.Holmes, R.Kashyap and R.Wyatt, "Physical Properties of Opitcal Fiber Sidetap Grating Filters: Free-Space Model ", *IEEE. J. Select. Topics Quantum Electron.* Vol.5, No.5, 1353(1999)
19. G.Nemova, J.Chauve, R.Kashyap, "Design of sidetap fiber Bragg grating filters", *Opt. Commun.*, vol. 259, no.2 pp.649-654, 2006
20. X Shu, L Zhang, I Bennion, "Sensitivity Characteristics of Long-Period Fiber Gratings," *J. Lightw. Technol.*, vol. 20, no.2, pp. 255-266, 2002
21. Byeong Ha Lee, Yu Liu, Sang Bae Lee, Sang Sam Choi, Joo Nyung Jang, ""*Opt. Lett.*, vol. 22, no. 23, pp.1769 -1771, 1997

Figure Captions

Figure 1 Phase matching conditions for TFBGs with tilted angles (a) <, (b) = and (c) >45°. (d) Image of fringes of a TFBG with large tilting angle. Note: in (a) $\mathbf{K_R}'$ and K_{core}' are for non phase match condition.

Figure 2 Three mode coupling regimes: (a) $\delta < \delta_{1c}$: backward cladding mode coupling; (b) $\delta_{1c} < \delta < \delta_{2c}$: radiation mode coupling; (c) $\delta > \delta_{2c}$: forward cladding mode coupling. Transmission spectra of TFBGs tilted at (d) 8° (showing cladding mode resonances with small spacing) and (e) 45° (showing smooth radiation loss profile). (f) 65° (showing resonances with larger spacing).

Figure 3 Transmission spectra of 65°-TFBG measured (a) around the phase match wavelength 820nm showing a radiation loss profile and (b) on the shorter wavelength side showing forward cladding mode coupling, and 69°-TFBG (c) measured around central wavelength 670nm, showing forward cladding mode coupling.

Figure 4 (a) A series of dual-peak resonances from 1200nm to 1700nm with near-even separation measured for 81°–TFBG. (b) The dual peaks are the coupling to the paired modes of two orthogonal polarization states.

Figure 5 Far field patterns of (a) 69°-TFBG fiber in air, (b) 69°-TFBG fiber in index matching gel and (c) the bare fiber sample. For all cases, the distance between the fiber tip and the screen was kept the same.

Figure 6 Thermal characteristics of ex-45° TFBGs. (a) Wavelength shifts of all dual peaks of the 69°-TFBG against temperature, showing almost no change with increasing temperature. (b) Wavelength shifts of two paired modes of the highest and lowest orders of 81°–TFBG against temperature, showing linear thermal responses with noticeably low thermal coefficients.

Figure 7 Strain responses of the 81°-TFBG: (a) linear and negative strain response for a peak at shorter wavelength side; (b) the strain induced wavelength shift depends on mode order and polarization.

Figure 8 SRI induced wavelength shifts in index range from 1.3 to 1.4 for the two peaks of 81°–TFBG close to 1200nm and 1700nm, respectively.
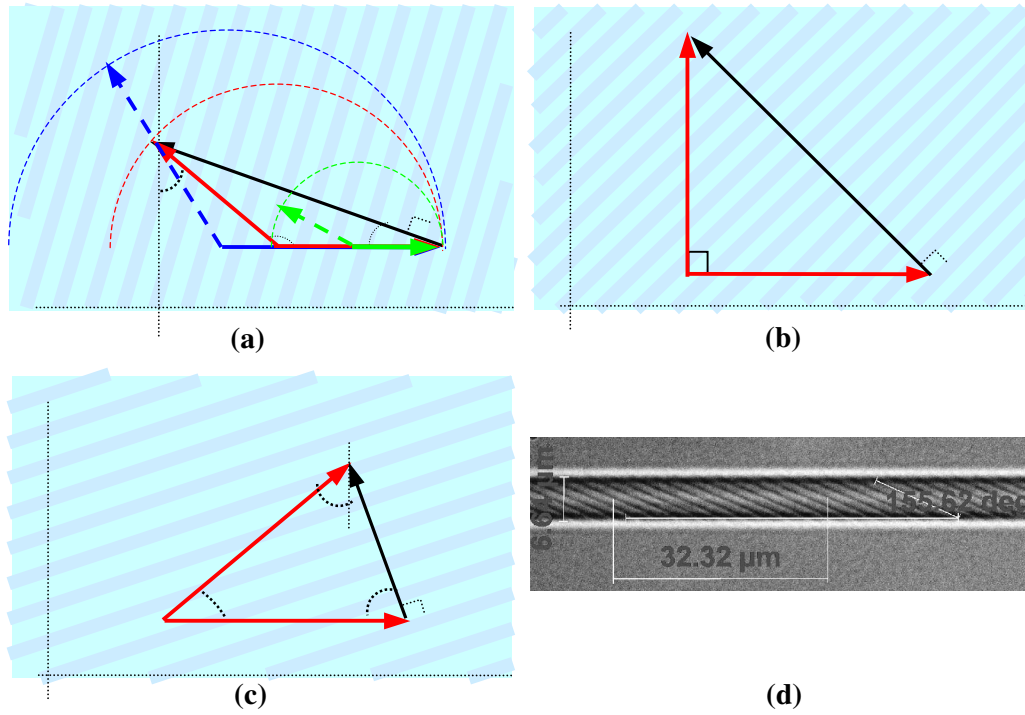
Figure 1

Figure 1 Phase matching conditions for TFBGs with tilted angles (a) <, (b) = and (c) >45°. (d) Image of fringes of a TFBG with large tilting angle. Note: in (a) $\mathbf{K_R}'$ and $\mathbf{K_R}''$ are for non phase match condition.
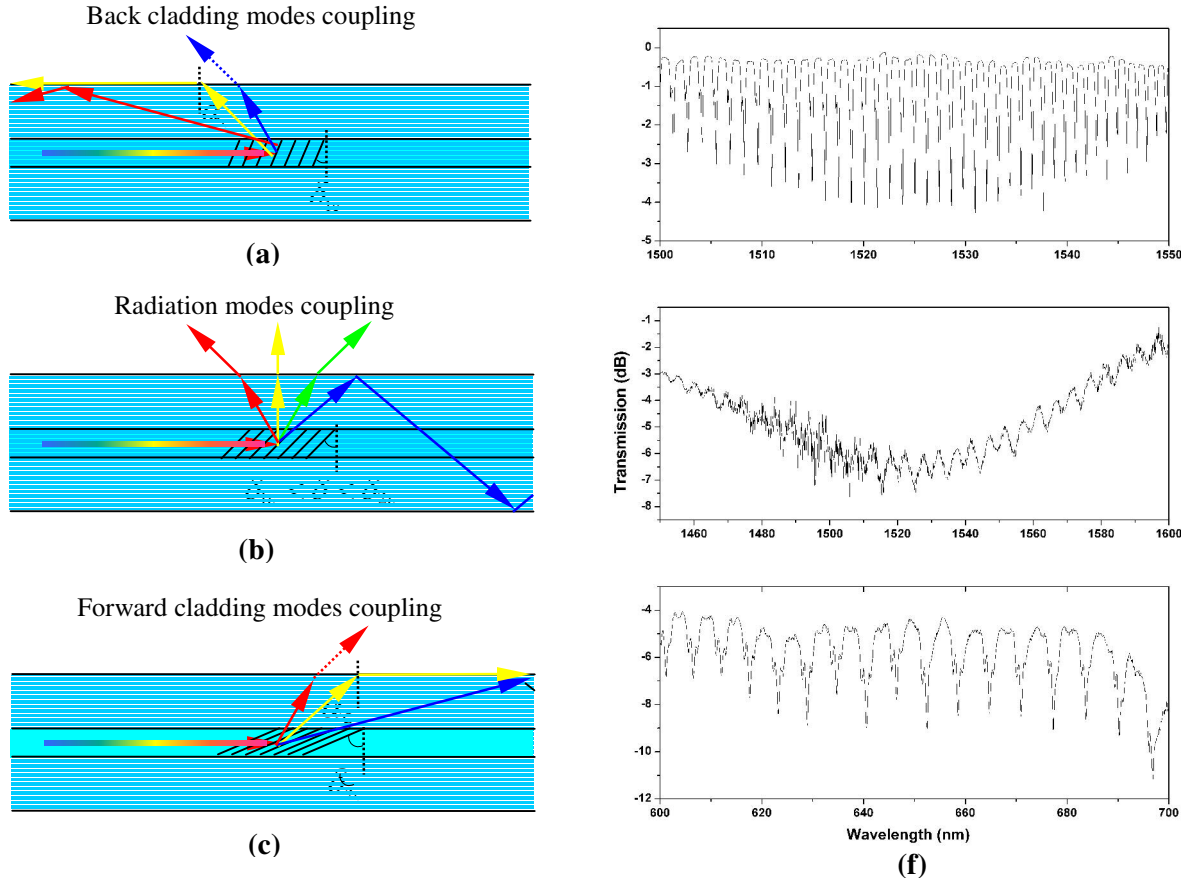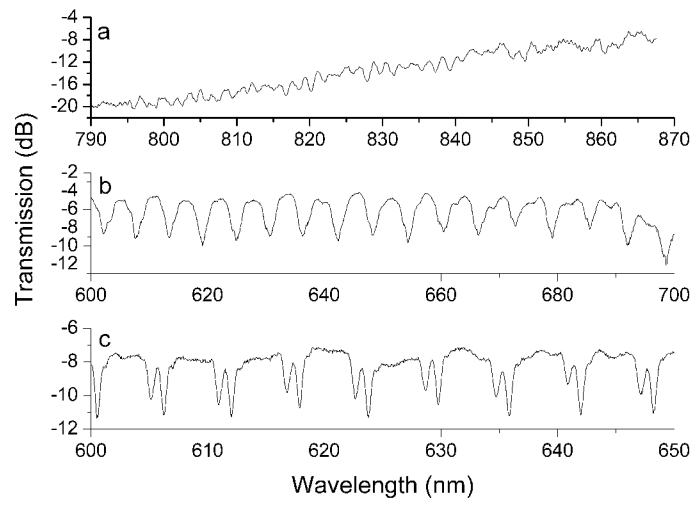
Figure 2 Three mode coupling regimes: (a) $\delta < \delta_{1c}$: backward cladding mode coupling; (b) $\delta_{1c} < \delta < \delta_{2c}$: radiation mode coupling; (c) $\delta > \delta_{2c}$: forward cladding mode coupling. Transmission spectra of TFBGs tilted at (d) 8° (showing cladding mode resonances with small spacing) and (e) 45° (showing smooth radiation loss profile). (f) 65° (showing resonances with larger spacing).

Figure 3 Transmission spectra of 65°-TFBG measured (a) around the phase match wavelength 820nm showing a radiation loss profile and (b) on the shorter wavelength side showing forward cladding mode coupling, and 69°-TFBG (c) measured around central wavelength 670nm, showing forward cladding mode coupling.
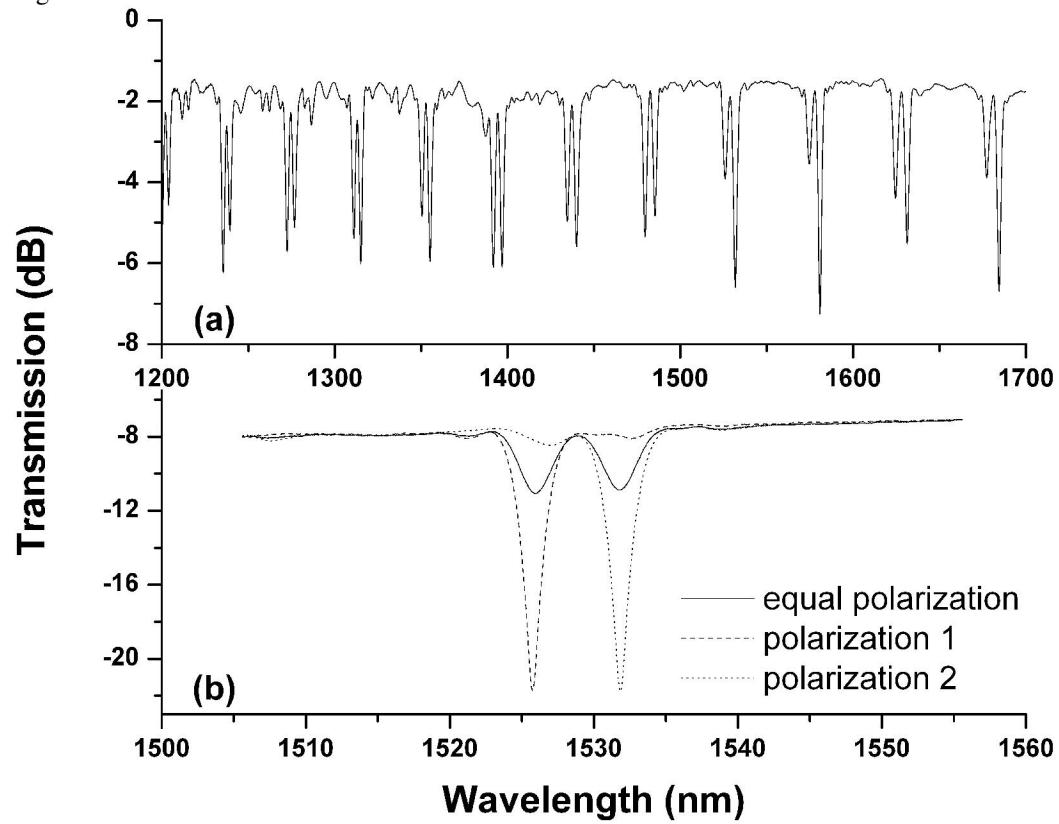
Figure 4

Figure 4 (a) A series of dual-peak resonances from 1200nm to 1700nm with near-even separation measured for 81°–TFBG. (b) The dual peaks are the coupling to the paired modes of two orthogonal polarization states.

Figure 5

(a)   **(b)**   **(c)**

Figure 5 Far field patterns of (a) 69°-TFBG fiber in air, (b) 69°-TFBG fiber in index matching gel and (c) the bare fiber sample. For all cases, the distance between the fiber tip and the screen was kept the same.
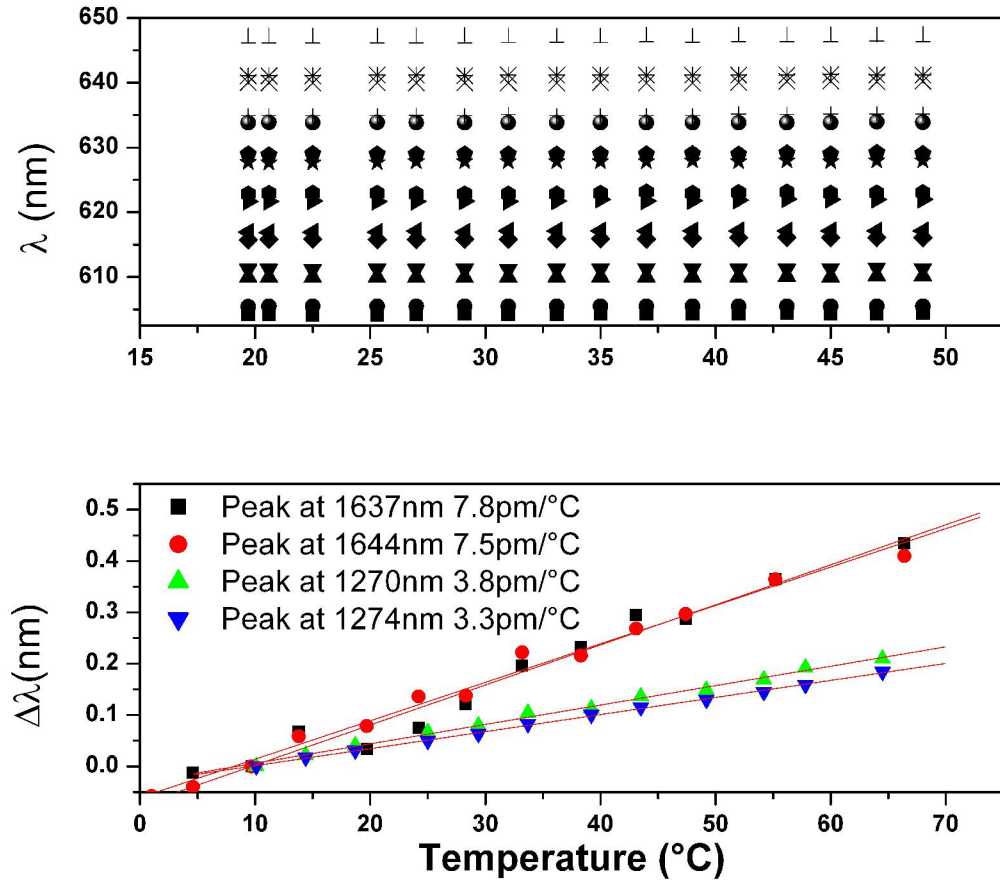
Figure 6

Figure 6 Thermal characteristics of ex-45° TFBGs. (a) Wavelength shifts of all dual peaks of the 69°-TFBG against temperature, showing almost no change with increasing temperature. (b) Wavelength shifts of two paired modes of the highest and lowest orders of 81°–TFBG against temperature, showing linear thermal responses with noticeably low thermal coefficients.
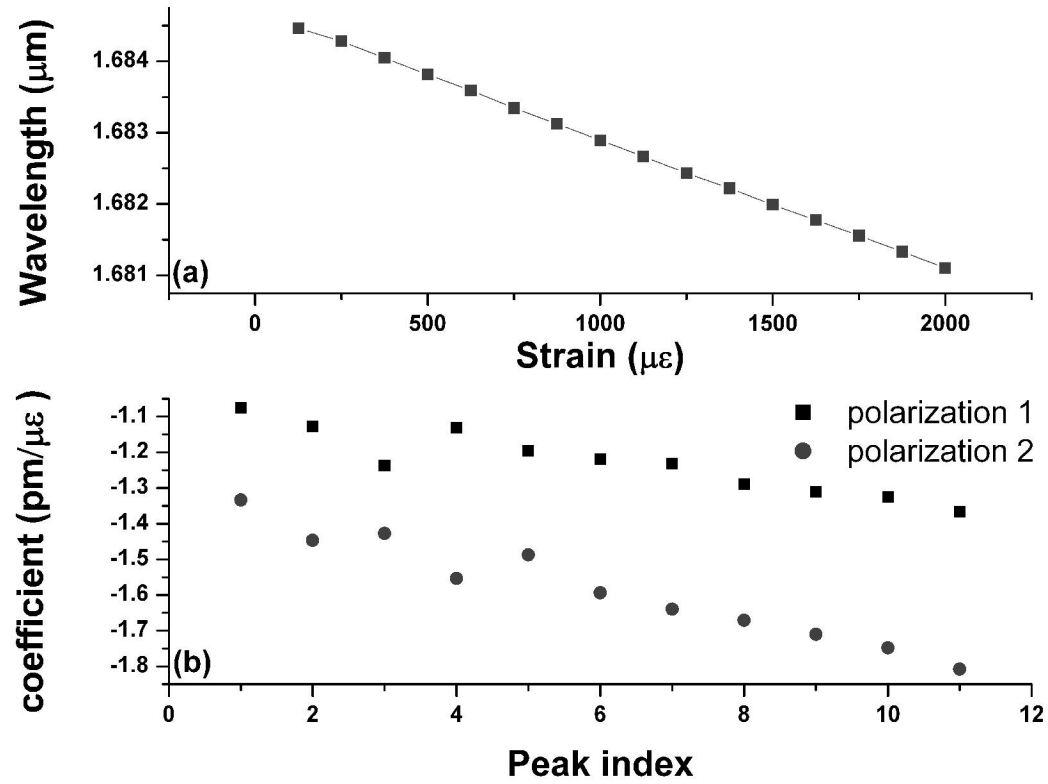
Figure 7

Figure 7 Strain responses of the 81°-TFBG: (a) linear and negative strain response for a peak at shorter wavelength side; (b) the strain induced wavelength shift depends on mode order and polarization.
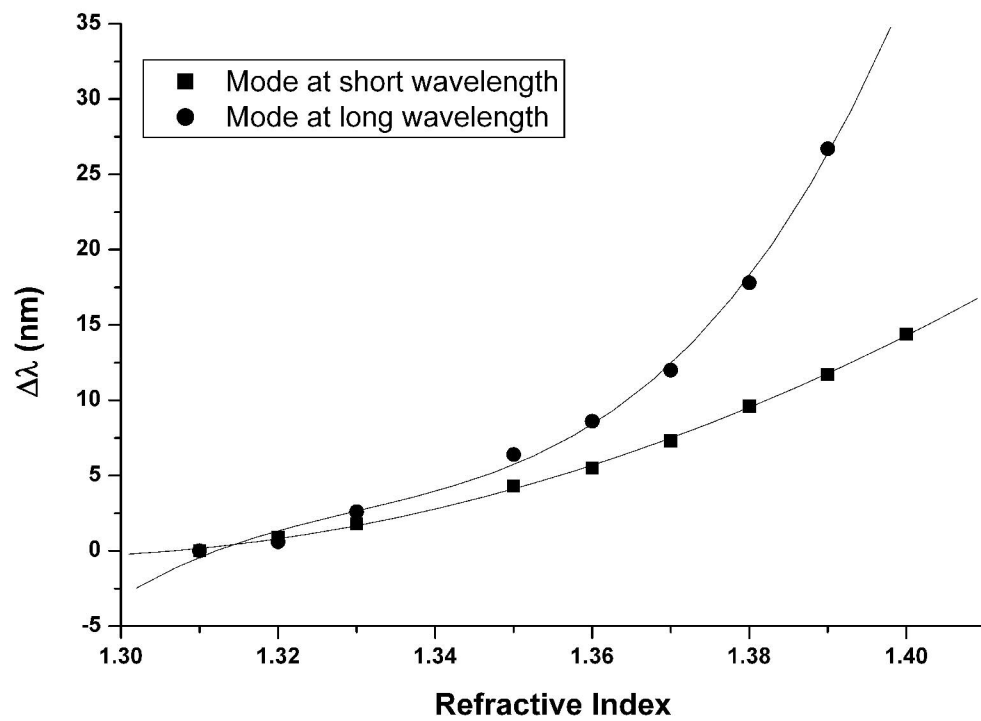
Figure 8

Figure 8 SRI induced wavelength shifts in index range from 1.3 to 1.4 for the two peaks of 81°−TFBG close to 1200nm and 1700nm, respectively.